

# Use of Coulometry to Assess the Protective Effect of Inhibitors

Alexander E. Kuzmak, Alexander V. Kozheurov, Larissa V. Frolova

IPCE RAS, 119991, Moscow, Leninsky Prospect, 31.

[akuzmak@yandex.ru](mailto:akuzmak@yandex.ru) [kuzmak@ipc.rssi.ru](mailto:kuzmak@ipc.rssi.ru)

## Abstract

This paper proposes a method for assessment of the protective effect of an amine corrosion inhibitor in *liquid* and *gas-vapor* hydrogen sulfide containing media using coulometric determination of corrosion products (hereinafter, CDCP). The kinetic regularities of the protective effect depending on the phase transformations of corrosion products on steel surface in H<sub>2</sub>S-containing media have been determined. Qualitative and quantitative analyses of the corrosion product composition have been performed by high-precision determination of sulfur- and oxygen-containing compounds of bi- and trivalent iron (Fe<sup>+2</sup>, Fe<sup>+3</sup> ions) within the range of 0.2 to 10 µg. The experimental technique using a glass-carbon indicator electrode-cell ensured high-precision registration of corrosion products (ions) at the sub-microcoulomb level (the discharge currents of the ions being determined are ~10<sup>-6</sup> A). Voltammetric measurements were used to identify sulfides and oxygen-containing corrosion products. The results of coulometric tests compared with gravimetric estimation proved the high information value of the suggested approach.

**Keywords:** coulometric method, detection of corrosion products, protective effect of inhibitor

## 1. Introduction

Studies on the protective mechanism of inhibitors of the hydrogen sulfide corrosion of iron by various physical methods (reflection electron diffraction, Auger and X-ray photoelectron spectroscopy, secondary ion mass spectrometry) have shown [1] that corrosion inhibition can occur upon inhibitor interaction with the “dense” corrosion product, *viz.*, fine-crystalline iron sulfide. As follows from the established surface layer structure, metal protection is effected by a complex iron compound containing inhibitor components and hydrosulfide groups that cover the sulfide crystals. Upon contact with a corrosive medium, this layer inhibits the recrystallization of fine-crystalline iron sulfide to a “loose” (coarse-crystalline) compound, thus ensuring a high protective effect. Thus, the kinetic region of the structure transition from a *dense* layer to a *loose* one, or *recrystallization region*, is of special interest in the experimental assessment of the inhibitor protective effect. In the current laboratory practice, the protective effects of inhibitors are generally evaluated by gravimetric and electrochemical methods. Matching between the results of both methods is either achieved by calibration or not achieved at all, particularly in the case of prolonged tests. The reason for this mismatch is that polarization affects the specimen in the course of data recording, thus distorting its real corrosion behavior and introducing uncertainty in the interpretation of the results. In essence, only the gravimetric method meets the direct measurement requirement. However, the gravimetric method is not free of known limitations, and besides, it is fundamentally unable to ensure the measurement of an important parameter of the corrosion process, *viz.*, the ion composition of the corrosion products.

The use of the advantages of gravimetry as a direct measurement method, along with elimination of its restrictions, allowed us to formulate the following requirements for the criterion, parameter, and measurement method that does not require any calibrations or assumptions [2]:

1. Quantitative determination of a direct corrosion parameter based on a fundamental physical law;
2. Elimination of effects of the measuring system on the specimen;
3. Clarity of *in situ* measurement results;
4. Accuracy, selectivity, high sensitivity, and efficiency of the measurements.

The above set of requirements can be satisfied by coulometry at a controlled potential; based on this method,

we developed a technique for the coulometric determination of corrosion products for studying the protective effect of inhibitors as described below.

## 2. Basis of the measurement methodology

The proposed approach is based on the use of Faraday's law, according to which the mass  $m$  (g) of a compound that undergoes the electrochemical conversion (in our case, corrosion products such as  $\text{Fe}^{2+}$  and  $\text{Fe}^{3+}$ ) is related to the consumed charge  $q$  (Cb) by the following equation:

$$m = K_e \cdot q = K_e \int I(t) dt \quad (1),$$

where:  $K_e = M/nF$  (g/Cb) is the electrochemical equivalent of the compound or reaction;  
 $I(t)$  is the discharge current of the ions being determined on the indicator electrode (IE) – *the measured parameter*;

$M$  is the molecular mass of the oxidized or reduced component (g);

$n$  is the number of electrons participating in the electrochemical conversion of one atom, ion, or molecule of the compound;

$F$  is the Faraday constant.

A CDCP experiment involves three main stages:

1. Exposure of the test specimen to a corrosive medium for a specified period of time.
2. Preparation of an aliquote containing the ions (corrosion products) for the coulometric analysis. At stage 2, the aliquotes with the ions (corrosion products) from the corrosive solution and from the metal surface are placed in a preserving solution in order to fix the oxidation states of the  $\text{Fe}^{2+}$  and  $\text{Fe}^{3+}$  ions.
3. Coulometric analysis of the aliquote: discharge of the ions (corrosion products) on an indicator electrode of the measuring system containing the reference (blank) electrolyte.

Coulometric analysis involves the determination of the compound being analyzed in a measuring cell at discharge potentials of the ions  $E_{\text{cat}}$ ,  $E_{\text{anod}}$  for the  $\text{Fe}^{2+} \leftrightarrow \text{Fe}^{3+}$  reactions and processing of the results.

The measuring cell represents the three-electrode potentiostatic scheme. A high-temperature glass carbon crucible that played the role of a measuring cell was used as the *indicator electrode* (IE). Carbon fiber was used as the auxiliary electrode. A silver chloride reference electrode was used. The coulometric measurements were carried out using an IPC – PRO electrochemical interface (manufactured by A.N.Frumkin Institute of Physical Chemistry and Electrochemistry of the Russian Academy of Sciences) equipped with specialized software.

## 3. Experimental

An amine inhibitor at 4 g/l concentration in a NACE medium (0.5 g/l NaCl + 250 mg/l  $\text{CH}_3\text{COOH}$  (pH=4), saturated with  $\text{H}_2\text{S}$  to 2000 mg/l) was used as the test object. The corrosive medium (250 ml) was placed in a 600-ml test vessel.

Three carbon steel specimens were placed in each the liquid and vapor-gas parts of the exposure space. Fresh steel specimens as well as fresh non-deaerated inhibited and non-inhibited media were used for each subsequent exposure interval. The specimens had the form of cylinders; the working area of each specimen available for coulometric and gravimetric measurements was  $8 \text{ cm}^2$ . We used the following sources of  $\text{Fe}^{2+,3+}$  ions (corrosion products): *dense* fine-crystalline corrosion products adsorbed on the metal surface; *loose* coarse-crystalline products adsorbed on the *dense* layer, as well as *loose* corrosion products transferred from the specimens from the *vapor-gas* medium to the *liquid* one during the exposure.

After exposure in the test medium for a specified time, corrosion products were removed from the specimen surfaces and preserved. *Loose* products were removed using a 4 M HCl washing solution at room temperature. *Dense* corrosion products were removed with an ammonium sulfosalicylate solution ( $\text{C}_7\text{H}_6\text{O}_6\text{S}$ ) with pH 4. The  $\text{Fe}^{2+,3+}$  ions from both washing solutions and from the liquid medium were determined on the IE (Table 1).

**Table 1.** Conditions of steel corrosion product determination by the CDCP method.

Ion	Fe <sup>2+,3+</sup> source	E, V	Reference solution in the IE
<b>Fe<sup>2+</sup></b>	NACE medium	0.43	1 M HCl in isopropanol + 0.3 mg/ml inhibitor + 0.1 mg/ml H <sub>2</sub> S
	<i>Loose</i>	0.77	Aqueous 0.1 M HCl + 4 mg/ml C <sub>7</sub> H <sub>6</sub> O <sub>6</sub> S
	<i>Dense</i>	0.77	Aqueous 0.1 M HCl
<b>Fe<sup>3+</sup></b>	NACE medium	0.13	Aqueous 0.1 M HCl + 12 mg/ml C <sub>7</sub> H <sub>6</sub> O <sub>6</sub> S + (0.1-0.4) µg/ml Fe <sup>2+</sup>
	<i>Loose</i>	0.13	Aqueous 0.1 M HCl + 4 mg/ml C <sub>7</sub> H <sub>6</sub> O <sub>6</sub> S
	<i>Dense</i>	0.13	Aqueous 0.1 M HCl + 12 mg/ml C <sub>7</sub> H <sub>6</sub> O <sub>6</sub> S + (0.1-0.4) µg/ml Fe <sup>2+</sup>

To identify the phase composition of the corrosion products (sulfur- and oxygen-containing iron compounds), voltammetric measurements were carried out from the corrosion potential  $E_{\text{corr}}$  to  $E = -1.8 \text{ V}$  and from  $E = -1.8 \text{ V}$  to  $E = 0 \text{ V}$  at potential scan rate  $v_{\text{scan}} = 5 \text{ mV/s}$ .

Figure 1 shows a cathodic voltammetric curve for carbon steel without an inhibitor under the conditions specified in Table 1.

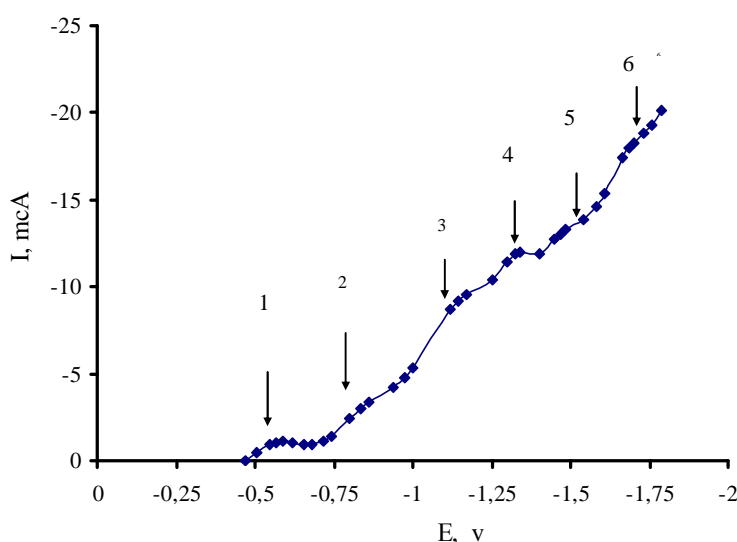


Fig. 1. Reference cathodic voltammetric curve for the reduction of corrosion products: 1.  $\text{Fe}^{2+} \rightarrow \text{Fe}^0$ ,  $E = -0.66 \text{ V}$ ; 2.  $\text{Fe}(\text{OH})_3 \rightarrow \text{Fe}(\text{OH})_2$ ,  $E = -0.87 \text{ V}$ ; 3.  $\text{Fe}(\text{OH})_2 \rightarrow \text{Fe}^0$ ,  $E = -1.19 \text{ V}$ ; 4.  $\text{FeS (dense)} \rightarrow \text{Fe}^0$ ,  $E = -1.34 \text{ V}$ ; 5, 6.  $\text{FeS (loose)} \rightarrow \text{Fe}^0$ ,  $E = -1.51 \text{ V}$  and  $E = -1.7 \text{ V}$ .

Tables 2 and 3 show the measurement results for the kinetics of the total mass loss of ions determined gravimetrically,  $\Sigma_{\text{gr}}$ , and by CDCP,  $\Sigma_{\text{CDCP}} = m_{\text{Fe}^{2+}} + m_{\text{Fe}^{3+}}$ , in the *liquid* and *vapor-gas* media. In evaluating the absolute mass loss, the additional corrosion products that were transferred from the *vapor-gas* phase to the *liquid* phase,  $\Delta_{\text{vg}} = \Sigma_{\text{CDCP}} - \Sigma_{\text{gr}}$ , were also taken into account.

**Table 2.** Total mass loss ( $\text{g/m}^2$ ) of specimens in inhibited and non-inhibited *liquid* media obtained by gravimetric and CDCP methods, taking  $\Delta_{\text{vg}}$  into account.

$t$ , hours	Without inhibitor			With inhibitor		
	Grav. $\Sigma_{\text{gr}}$	CDCP $\Sigma_{\text{CDCP}}$	$\Delta_{\text{vg}}$	Grav. $\Sigma_{\text{gr}}$	CDCP $\Sigma_{\text{CDCP}}$	$\Delta_{\text{vg}}$
0.75	0.52	0.48	0	0.09	0.07	0
1.5	3.61	3.27	0.34	0.18	0.21	0
3	7.26	6.58	0.68	0.60	0.59	0
6	14.48	14.00	0.48	0.84	0.82	0
12	31.97	31.42	0.55	0.84	0.83	0
18	29.71	28.42	1.29	1.62	1.52	0
19.5	29.07	26.50	2.57	3.61	3.63	0
21	37.46	33.55	3.91	12.48	12.31	0
24	45.98	44.26	1.72	15.62	15.08	0
120	88.87	88.11	0.76	19.07	19.00	0
240	103.54	102.88	0.66	20.87	20.99	0
360	108.42	107.21	1.21	62.34	63.66	0

**Table 3.** Mass loss ( $\text{g/m}^2$ ) of specimens in inhibited and non-inhibited *vapor-gas* media obtained by gravimetric and CDCP methods.

$t$ , hours	Without inhibitor			With inhibitor		
	Grav.	CDCP	$\Delta_{\text{vg}}$	Grav.	CDCP	$\Delta_{\text{vg}}$
	$\Sigma_{\text{gr}}$	$\Sigma_{\text{CDCP}}$		$\Sigma_{\text{gr}}$	$\Sigma_{\text{CDCP}}$	
0.75	0.03	0.01	0	0	0	0
1.5	0.66	1.02	0.36	0	0	0
3	1.30	2.00	0.70	0	0	0
6	3.74	4.25	0.1	0	0	0
12	5.41	5.92	0.51	0	0	0
18	6.94	8.27	1.33	0	0	0
19.5	9.20	11.70	2.50	0	0	0
21	12.36	16.18	3.82	0	0	0
24	12.99	14.61	1.69	0	0	0
120	18.14	18.83	0.69	11.98	11.99	0
240	34.01	34.72	0.71	18.00	17.60	0
360	63.89	65.03	1.14	30.88	31.30	0

### 3.1. CDCP measurements in *liquid* medium

As one can see from Tables 2 and 3, the results of integral kinetics measurements by both methods are in good agreement, taking the  $\Delta_{\text{vgm}}$  in non-inhibited medium into account.

For illustration purposes, Figures 2 and 3 show the results of mass loss kinetics measurements by the CDCP method in the *liquid* medium for  $t = 0 - 24$  h and  $t = 0 - 360$  h exposures.

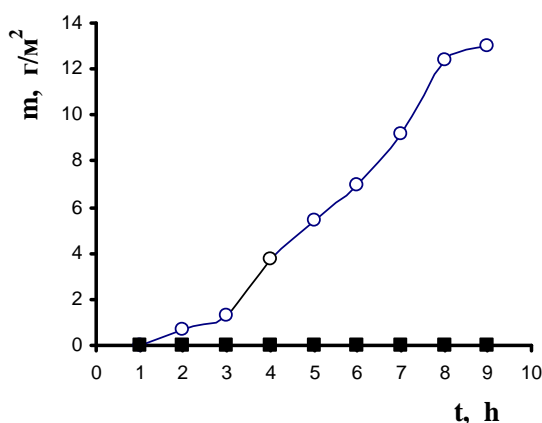


Fig. 2.

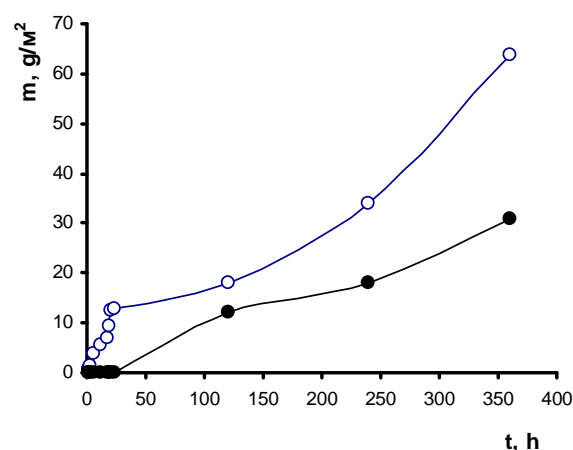


Fig. 3.

Mass loss kinetics in the *liquid* medium in the tests for 24 and 360 hours:

● – with inhibitor; ○ – without inhibitor, respectively

Table 4 presents the kinetics of the total amounts of the corrosion products ( $\text{Fe}^{2+} + \text{Fe}^{3+}$ ) on the specimen surface,  $\Sigma_s$ , and in the *liquid* medium,  $\Sigma_{lm}$ , as well as their ratios:  $\sigma_{\text{Fe}} = \Sigma_s / \Sigma_{lm}$ . **Table 4.** Kinetics of the amount of combined corrosion products and their ratio  $\sigma_{\text{Fe}}$  obtained by CDCP method.

$t$ , h	$\Sigma_s$ on the surface	$\Sigma_{lm}$ in the liquid medium	$\sigma_{\text{Fe}}$
0.75	0	0.01	0
1.5	0.47	0.19	2.5
3	0.77	0.53	1.5
6	1.95	1.99	1.0
12	2.72	2.69	1.0
18	3.40	3.54	1.0
19.5	4.23	4.97	0.8
21	5.64	6.72	0.8
24	6.51	6.48	1.0
120	10.99	7.15	1.5
240	15.15	19.57	0.8
360	8.58	56.45	0.2



As one can see from Table 4, the corrosion process in the *liquid* non-inhibited medium is controlled by a “protective” layer of corrosion products on the metal surface. This layer is formed within the first three hours of the test. This period is followed by regions of slower (from 6 to 18 h and from 24 to 120 h,  $\sigma_{\text{Fe}} \geq 1.0$ ) and faster corrosion (from 18 to 24 h and from 120 to 360 h,  $\sigma_{\text{Fe}} \leq 0.8$ ). On transition from a region with slower corrosion to a region with faster corrosion, the layer of corrosion products reaches a “critical” thickness and starts to undergo mechanical degradation. A fraction of the corrosion products are transferred from the specimen surface to the *liquid* medium. During this period, an increase in the metal mass loss is observed, which characterizes the recrystallization of *dense* iron sulfide. According to CDCP data, fast accumulation of *loose* products in  $\text{Fe}^{2+}$  form ( $\sim 85\%$ ) and in oxidized  $\text{Fe}^{3+}$  form ( $\sim 10\text{--}15\%$ ) occurs. However, the amount of *dense* products is at the detection level. The sulfide nature of the *loose*  $\text{Fe}^{2+}$  products is confirmed by the cathodic voltammetric curve (Fig. 4) that contains a signal of the reduction of a mixture of various sulfides, which is by an order of magnitude higher than the signal of the reduction of oxygen-containing  $\text{Fe}^{3+}$  compounds.

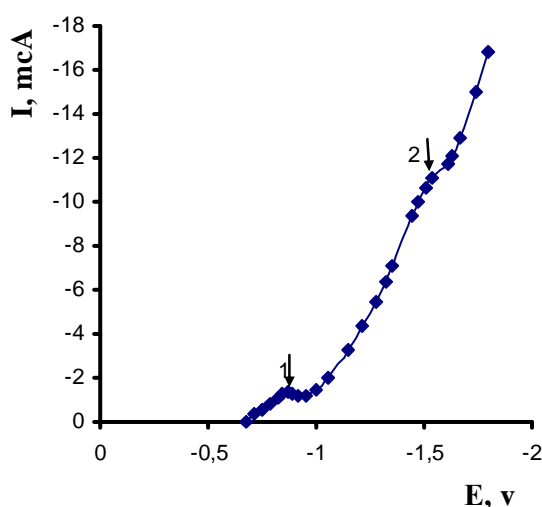


Fig. 4. Cathodic voltammetric curve of reduction of corrosion products in the liquid non-inhibited medium after exposure for 21 h: 1.  $\text{Fe}(\text{OH})_3 \rightarrow \text{Fe}(\text{OH})_2$ ,  $E = -0.87$  V; 2.  $\text{FeS} (\text{loose}) \rightarrow \text{Fe}^0$ ,  $E = -1.58$  V.

As shown previously (Fig. 2), the protective effect in inhibited *liquid* medium for 24 h amounted to  $\sim 100\%$ . However, it follows from further studies that the start of recrystallization is accompanied by the formation of micro amounts of only *loose*  $\text{Fe}^{2+}$  compounds in the form of sulfides that are partially transferred to the *liquid medium* (Table 5).

**Table 5.** Kinetics of the phase composition of corrosion products in the *liquid* inhibited medium, g/m<sup>2</sup>.

t, h	Fe <sup>2+</sup> compounds		Fe <sup>3+</sup> compounds		Fe <sup>2+</sup> compounds		Fe <sup>3+</sup> compounds	
	dense	loose	dense	loose	dense	loose	dense	loose
0.75	0	0.28	0	0.20	0.07	0	0	0
1.5	0	3.16	0	0.45	0.16	0	0	0.05
3	0.10	6.07	0	1.09	0.50	0	0	0.09
6	0.06	12.89	0	1.53	0.63	0	0	0.19
12	0.05	29.01	0	2.91	0.55	0.06	0	0.22
18	0.29	27.13	0	2.29	0.47	0.32	0.46	0.27
19.5	0.27	26.31	0	2.49	0.43	2.56	0.27	0.37
21	0.12	33.34	0	4.00	0.04	11.05	0.11	1.11
24	0.17	42.79	0	3.02	0.17	13.42	0	1.49

Figure 5 demonstrates the cathodic voltammetric curve of corrosion products in the *liquid* inhibited medium.

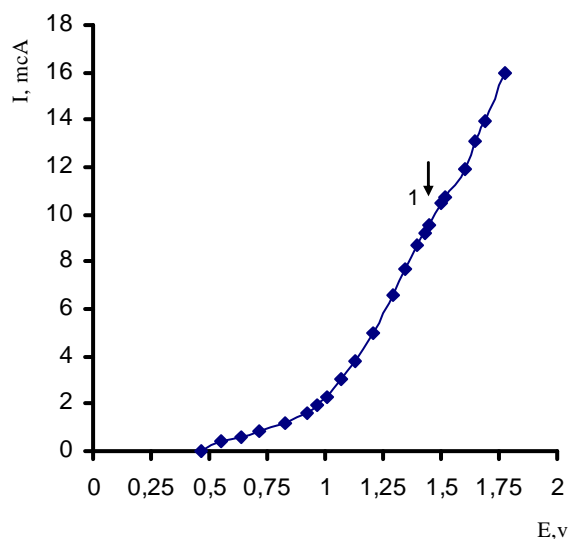


Fig. 5. Cathodic voltammetric curve of reduction of corrosion products in the *liquid* inhibited medium after exposure for 240 h: 1. FeS (*loose*) → Fe<sup>0</sup>, E = -1.55 V.



Thus, the loss of protective effect can be detected by determining micro amounts of *loose*  $\text{Fe}^{2+}$  compounds both on the metal surface and in the *liquid* medium.

### 3.2. CDCP measurements in vapor-gas medium

As shown in Figures 6 and 7, the corrosion process in the *vapor-gas* phase without an inhibitor contains regions where the mass loss kinetics is stabilized, *i.e.*, 12 – 19.5 h and 120 – 360 h, and regions where it increases, *i.e.*, 0.75 – 12 h and 19.5 – 120 h.

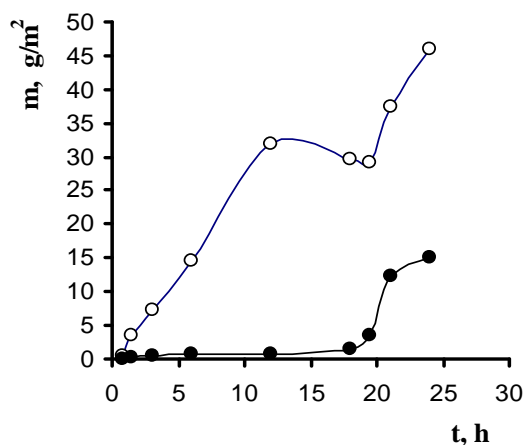


Fig. 6.

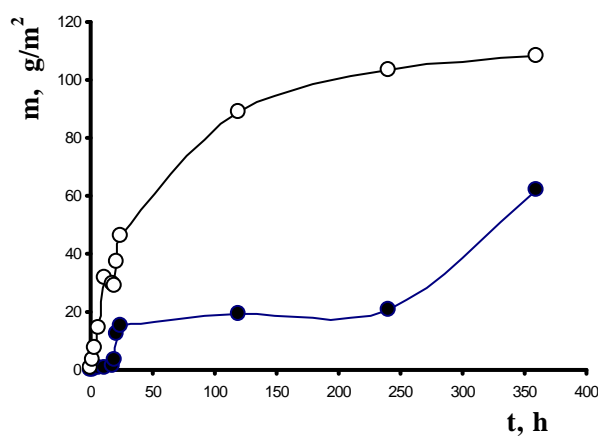


Fig. 7.

Kinetics of  $m(\text{Fe}^{2+} + \text{Fe}^{3+})$  mass loss in the *vapor-gas* medium during exposure for 24 h and 360 h:

● – with inhibitor; ○ – without inhibitor, respectively

Table 6 shows the kinetics of the phase composition of corrosion products for the *dense* and *loose* phase layers in the *vapor-gas* medium.

**Table 6.** Kinetics of the phase composition of corrosion products in the *vapor-gas* medium, /m<sup>2</sup>.

<i>t</i> , h	Non-inhibited medium				Inhibited medium			
	Fe <sup>2+</sup> compounds		Fe <sup>3+</sup> compounds		Fe <sup>2+</sup> compounds		Fe <sup>3+</sup> compounds	
	dense	loose	dense	loose	dense	loose	dense	loose
0.75	0	0.28	0	0.20	0.07	0	0	0
1.5	0	3.16	0	0.45	0.16	0	0	0.05
3	0.10	6.07	0	1.09	0.50	0	0	0.09
6	0.06	12.89	0	1.53	0.63	0	0	0.19
12	0.05	29.01	0	2.91	0.55	0.06	0	0.22
18	0.29	27.13	0	2.29	0.47	0.32	0.46	0.27
19.5	0.27	26.31	0	2.49	0.43	2.56	0.27	0.37
21	0.12	33.34	0	4.00	0.04	11.05	0.11	1.11
24	0.17	42.79	0	3.02	0.17	13.42	0	1.49
120	1.77	4.37	8.55	4.28	0.46	6.65	0	1.89
240	12.17	75.58	10.49	4.64	1.82	17.44	0	1.73
360	10.35	8.90	7.15	12.02	1.84	8.08	0.36	2.06

One can see from Figures 6 and 7 and from Table 6 that the regions of mass loss in the medium are presumably due to recrystallization of *dense* sulfide, since the amount of *loose* Fe<sup>2+</sup> products exceeds the amount of *dense* Fe<sup>2+</sup> products by two orders. Corrosion is hindered due to a 5-10-fold increase in the amount of *dense* corrosion products in the form of Fe<sup>2+</sup>, while the amount of *loose* products on these areas remains almost unchanged. It follows from the cathodic voltammetric curves obtained in the slow-down regions (Fig. 8), *e.g.*, after 18 hours, that the *dense* Fe<sup>2+</sup> products formed in the vapor-gas phase without an inhibitor are oxygen-containing compounds. A signal with a maximum at *E* = - 0.95 V is observed which combines the reduction regions of oxygen-containing Fe<sup>2+</sup> and Fe<sup>3+</sup> compounds; a signal from sulfides is almost not observed here

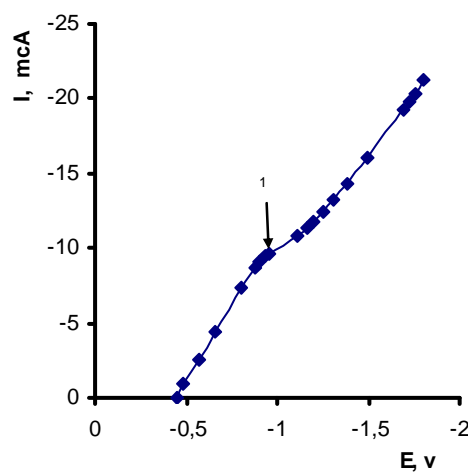


Fig. 8. Cathodic voltammetric curve of reduction of corrosion products in the vapor-gas non-inhibited medium after exposure for 18 h: 1.  $\text{Fe}(\text{OH})_3 \rightarrow \text{Fe}(\text{OH})_2$ ,  $\text{Fe}(\text{OH})_2 \rightarrow \text{Fe}^0$ ,  $E = -0.95 \text{ V}$ .

Figures 9a and 9b show the kinetics of the inhibitor protective effect ( $Z$ , %) in the *vapor-gas* medium: a) from 0 to 25 h; b) from 25 to 360 h.

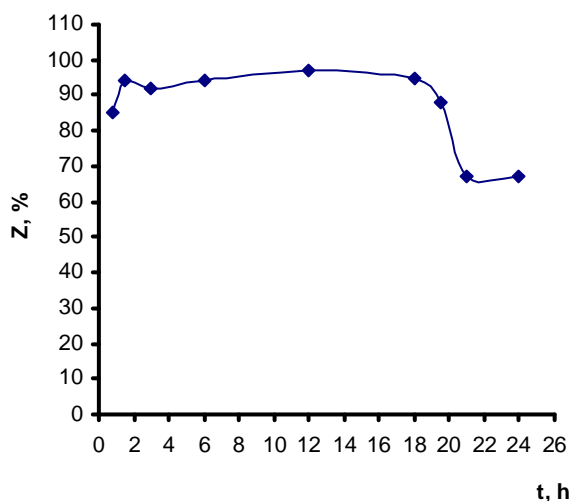


Fig. 9a.

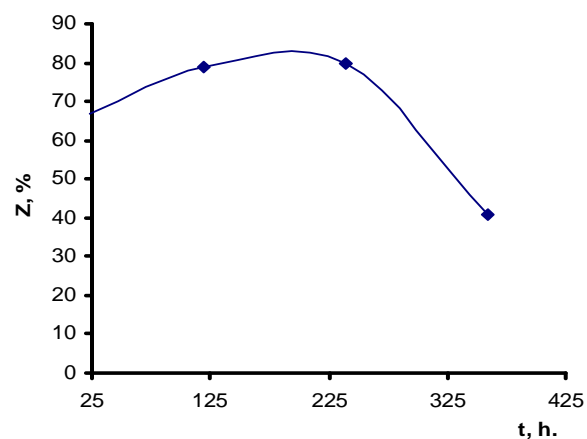


Fig. 9b.

Kinetics of  $(\text{Fe}^{2+} + \text{Fe}^{3+})$  integral mass loss in the *vapor-gas* medium during exposure for 25 h (9a) and 360 h (9b), respectively.

The composition of the corrosion products for 6-12 h exposure is shown on the voltammetric curve (Fig. 10) where one can see signals from *dense* iron sulfide and oxygen-containing  $\text{Fe}^{3+}$  compounds.

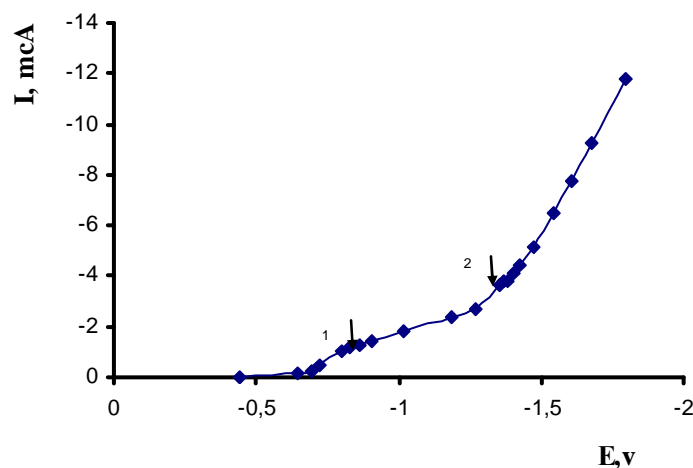


Fig. 10. Cathodic voltammetric curve for the reduction of corrosion products in the *vapor-gas* inhibited medium after exposure for 6 h: 1.  $\text{Fe}(\text{OH})_3 \rightarrow \text{Fe}(\text{OH})_2$ ,  $E = -0.84 \text{ V}$ ; 2.  $\text{FeS} (\text{dense}) \rightarrow \text{Fe}^0$ ,  $E = -1.35 \text{ V}$ .

Thus, the effect of the aforementioned *dense* oxygen-containing corrosion products is obvious, since, in addition to a shift of the iron dissolution signal, a signal of oxidation  $\text{Fe}(\text{OH})_2 \rightarrow \text{Fe}(\text{OH})_3$  at  $E = -0.84 \text{ V}$  is also observed. It also follows from Table 6 that, after 12 h of exposure, the phase composition of the corrosion products changes as follows:  $\sim 10\%$  of *dense*  $\text{Fe}^{2+}$  products is converted to *loose* products, while the total amount of  $\text{Fe}^{2+}$  products is the same as that after exposure for 6 h. This change in the phase composition suggests that sulfide *recrystallization* starts, which stimulates corrosion acceleration. In the period from 12 to 24 h, the content of *dense*  $\text{Fe}^{2+}$  products on the specimen surface decreases by an order. The amount of *loose*  $\text{Fe}^{2+}$  products increases by approximately the same value. Exposure to oxygen results in the formation of *dense* oxygen-containing  $\text{Fe}^{3+}$  compounds. However, the latter provide no protective effect; hence, it may be assumed (Table 6) that only *dense* oxygen-containing  $\text{Fe}^{2+}$  compounds have protective ability. The recrystallization is mostly completed by 21 hours of exposure. During this process, the metal mass loss increases 15-fold, whereas the protective effect decreases from 95% to 67% (Fig. 9a). However, the kinetics of the subsequent corrosion process does not repeat that of the non-protected metal. The process slows down in the period from 24 to 240 h (Fig. 6, Table 3), so the mass loss increases no more than 1.4-fold. During this period, the amount of *solid*  $\text{Fe}^{2+}$  products again increases, whereas the amount of *loose* products increases only a little (Table 6). The efficiency of metal protection during this period is rather high, *i.e.*, 70-80% (Fig. 9b). However, the protection that is achieved is not related to inhibitors, as data of the cathodic voltammetric curve recorded after 120 h suggest (Fig. 11).

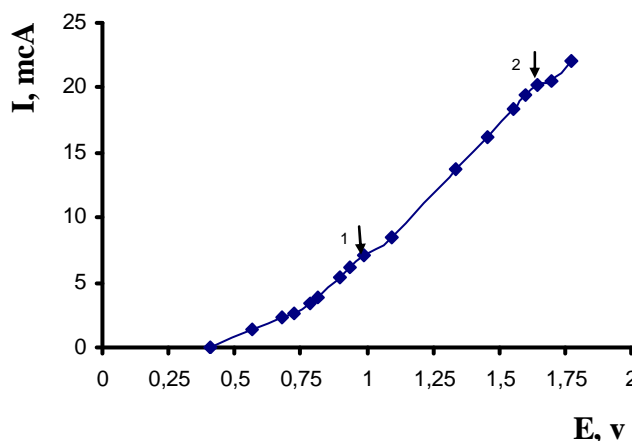


Fig. 11. Cathodic voltammetric curve for the reduction of corrosion products in the *vapor-gas inhibited* medium after exposure for 120 h: 1.  $\text{Fe}(\text{OH})_3 \rightarrow \text{Fe}(\text{OH})_2$ ,  $\text{Fe}(\text{OH})_2 \rightarrow \text{Fe}^0$ ,  $E = -0.98$  V; 2.  $\text{FeS (loose)} \rightarrow \text{Fe}^0$ ,  $E = -1.65$  V.

These results show that metal protection is provided by a layer of *dense* oxygen-containing  $\text{Fe}^{2+}$  compounds.

#### 4. Conclusions

1. In this paper we propose a method for the coulometric determination of corrosion products (CDCP) for assessment of the protective effect of corrosion inhibitors in *liquid* and *vapor-gas*  $\text{H}_2\text{S}$ -containing media.
2. The kinetic regularities of changes in the inhibitor protective effect depending on the phase transformations of sulfur- and oxygen-containing compounds on the metal surface have been determined.
3. Qualitative and quantitative analyses of the corrosion product composition have been performed by high-precision determination of sulfur- and oxygen-containing compounds of bi- and trivalent iron.
4. The main feature of the inhibitor protective effect has been identified: kinetic *recrystallization region* of fine-crystalline to coarse-crystalline sulfide.

#### ACKNOWLEDGMENTS

The authors are grateful to Prof. Y. I. Kuznetsov and Dr. N. N. Andreev for valuable comments.

#### REFERENCES

- [1]. "The Formation of Protective Films on Iron under the Action of the Inhibitor IFHANGAZ-1 in an Aqueous Solution Saturated with Hydrogen Sulfide", Rozenfel'd I.L., Bogomolov D.B., Gorodetsky A.E., Kazansky L.P., Frolova L.V., Shamova L.I. " *Zashchita metallov*", 18, 2, pp. 163-168, 1982..
- [2]. "Coulometric Estimation of Corrosion Rate of Carbon Steel", Kuzmak A.E., Kozheurov A.V. " *Protection of Metal and Physical Chemistry of Surfaces*", 40, 3, pp. 315 – 320, 2004.